FERMILAB-CONF-09-368-E

MiniBooNE Oscillation Results

Zelimir Djurcic (for the MiniBooNE Collaboration)
Department of Physics, Columbia University, New York, NY 10027, USA

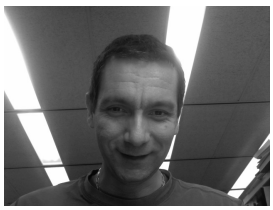

These proceedings summarize the MiniBooNE $\nu_\mu \rightarrow \nu_e$ results, describe the first $\bar{\nu}_\mu \rightarrow \bar{\nu}_e$ result, and current analysis effort with the NuMI neutrinos detected in the MiniBooNE detector.

1 Introduction

Motivated by the LSND observation of an excess of observed $\bar{\nu}_e$ events above Monte Carlo prediction in a $\bar{\nu}_\mu$ beam [1], the MiniBooNE experiment was designed to test the neutrino oscillation interpretation of the LSND signal in both neutrino and anti-neutrino modes. MiniBooNE has approximately the same L/E_ν as LSND, where L is the neutrino travel distance and E_ν is the neutrino energy. However, the MiniBooNE experiment is constructed with an order of magnitude higher baseline and energy. Due to the higher energy and different event signature, MiniBooNE systematic errors are completely different from LSND errors.

2 MiniBooNE Neutrino Results

The MiniBooNE collaboration has performed a search for $\nu_\mu \rightarrow \nu_e$ oscillations with 6.486×10^{20} protons on target (POT), the results of which showed no evidence of an excess of ν_e events for neutrino energies above 475 MeV [2,3]. Fig. 1 shows reconstructed E_ν distribution of ν_e CCQE candidates (left). The right panel of Fig. 1 shows the difference between the data and predicted backgrounds as a function of reconstructed neutrino energy. Table 1 shows observed data and predicted background event numbers in three E_ν bins. The total background is broken down into intrinsic ν_e and ν_μ induced components. The ν_μ induced background is further broken down into its separate components. Despite having observed no evidence for oscillations above 475 MeV, the MiniBooNE $\nu_\mu \rightarrow \nu_e$ search observed a sizable excess (128.8±43.4 events) at low energy, between 200-475 MeV [3]. Although the excess is incompatible with LSND-type oscillations, several hypotheses, including sterile neutrino oscillations with CP violation [4], anomaly-mediated neutrino-photon coupling [5], and others [6,7,8,9], have been proposed that provide a possible explanation for the excess itself. In some cases, these theories offer the possibility of reconciling the

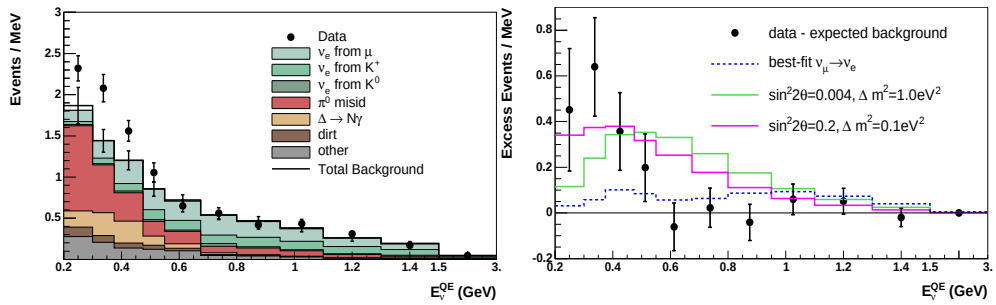

Figure 1: Left: Reconstructed E_ν distribution of ν_e CCQE candidates in MiniBooNE neutrino running. The data is shown as the points with statistical error. The background prediction is shown as the histogram with systematic errors. Right: The difference between the data and predicted backgrounds as a function of reconstructed neutrino energy. The error bars include both statistical and systematic components. Also shown in the figure are expectations from the best oscillation fit and from neutrino oscillation parameters in the LSND allowed region.

E_ν[GeV]	0.2-0.3	0.3-0.475	0.475-1.25
Total Bkgd	186.8±26	228.3±24.5	385.9±35.7
ν_e induced	18.8	61.7	248.9
ν_μ induced	168	166.6	137
NC π^0	103.5	77.8	71.2
NC $\Delta \rightarrow N\gamma$	19.5	47.5	19.4
Dirt	11.5	12.3	11.5
Other	33.5	29	34.9
Data	232	312	408
Data-MC	45.2±26	83.7±24.5	22.1±35.7
Significance	1.7σ	3.4σ	0.6σ

Table 1: Observed data and predicted background event numbers in three E_ν bins. In the top rows, the total background is separated into the intrinsic ν_e and ν_μ induced components. In the middle rows, the ν_μ induced background is further broken down into its separate components.

MiniBooNE ν_e excess with the LSND $\bar{\nu}_e$ excess. Assuming no CPT or CP violation, the lack of the excess at higher energies allowed MiniBooNE to exclude the LSND excess interpreted as two-neutrino oscillations at $\Delta m^2 \sim$ 0.1-100 eV^2 at 98% CL [10].

3 MiniBooNE Anti-neutrino Results

In December 2008, the MiniBooNE Collaboration also reported initial results from a search for $\bar{\nu}_\mu \rightarrow \bar{\nu}_e$ oscillations [11], using a data sample corresponding to 3.386×10^{20} POT. The data are consistent with background prediction across the full range of reconstructed neutrino energy, $200 < E_\nu < 3000$ MeV: 144 electron-like events have been observed in this energy range, compared to an expectation of 139.2 ± 17.6 events. Fig. 2 (left) shows reconstructed E_ν distribution of ν_e CCQE candidates. Table 2 shows observed data and predicted background event numbers in two E_ν bins. Fig. 2 (right) shows the expected sensitivity and the limit to $\bar{\nu}_\mu \rightarrow \bar{\nu}_e$ oscillations from fit to the energy distribution, E_ν. No significant excess of events has been observed, both at low energy, 200-475 MeV, and at high energy, 475-1250 MeV, although the data are inconclusive with respect to antineutrino oscillations at the LSND level. The 475-675 MeV region shows the data fluctuation of a 2.8 σ above the predicted background, resulting with the MiniBooNE $\bar{\nu}_\mu \rightarrow \bar{\nu}_e$ oscillation limit being worse than the sensitivity at lower Δm^2. These preliminary results, with the excess observed in neutrino mode and the lack of excess in anti-neutrino mode, are surprising and suggest that there may be an unexpected difference between neutrino and anti-neutrino properties.

It is possible to perform a first comparison of neutrino and anti-neutrino results in the low energy region, 200-475 MeV, and ask how consistent are the anti-neutrino and neutrino excesses under different assumptions (models). For example, it may be speculated that the excess of

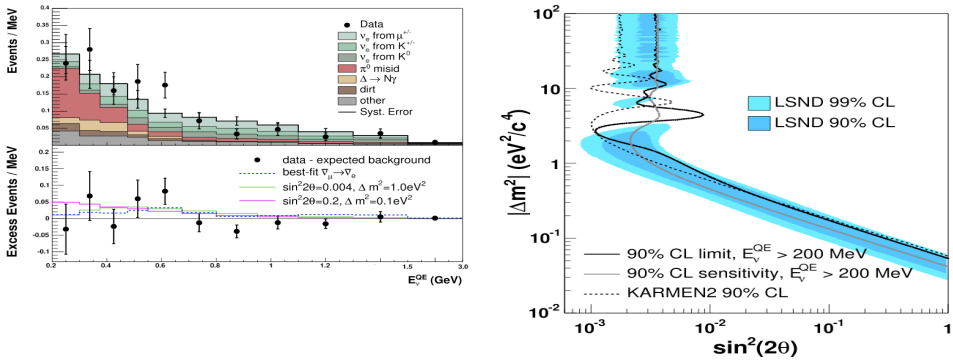

Figure 2: Left Top: Reconstructed E_ν distribution of ν_e CCQE candidates in MiniBooNE anti-neutrino running. Left Bottom: The difference between the data and predicted backgrounds as a function of reconstructed neutrino energy. The error bars include both statistical and systematic components. Also shown in the figure are expectations from the best oscillation fit and from neutrino oscillation parameters in the LSND allowed region. Right: Expected sensitivity and the limit to $\bar{\nu}_\mu \rightarrow \bar{\nu}_e$ oscillations from fit to the energy distribution, E_ν.

E_ν[GeV]	0.2-0.475	0.475-1.25
Total Bkgd	61.5±11.7	57.8±10.0
$\overset{(-)}{\nu}_e$ induced	17.7	43.1
$\overset{(-)}{\nu}_\mu$ induced	42.6	14.5
NC π^0	24.6	7.2
NC $\Delta \rightarrow N\gamma$	6.6	2.0
Dirt	4.7	1.9
Other	6.7	3.4
Data	61	61
Data-MC	-0.5±11.7	3.2±10.0
Significance	-0.04σ	0.3σ

Table 2: Observed data and predicted background event numbers in two E_ν bins. In the top rows, the total background is separated into the intrinsic $\overset{(-)}{\nu}_e$ and $\overset{(-)}{\nu}_\mu$ induced components. In the middle rows, the $\overset{(-)}{\nu}_\mu$ induced background is further broken down into its separate components.

events in the neutrino mode comes from an interaction resulting in an event rate proportional to the number of protons on the MiniBooNE target (POT). The number of protons on target in neutrino and antineutrino mode is 6.486×10^{20}, and 3.386×10^{20}, respectively. If the excess of 128.8±43.4 events observed in the neutrino mode is scalable with number of protons, then one would expect about $128.8\times(3.386\times10^{20}/6.486\times10^{20}) = 67$ excess events in anti-neutrino mode. However, such excess was not observed. Statisticaly, the simplest comparison is in the form a two bin (one bin for ν, another one for $\bar{\nu}$ data and Monte Carlo) χ^2 test for each assumption with corresponding errors being statistical only, and with systematic errors fully correlated or uncorrelated. Table 3 gives a χ^2 probability assuming one degree of freedom for testing the following hypotheses as an explanation of the low energy events in neutrino and anti-neutrino modes: the excess comes from an interaction resulting in the event rate proportional to the number of protons on the MiniBooNE target (POT scaled), from a neutral current process with same cross-section for neutrino and anti-neutrino interaction (Same ν,$\bar{\nu}$ NC), from underestimated neutral current π^0 background (NC π^0 scaled), from underestimated total background (Bkgd scaled), from an underestimate of kaon flux in at low energies (Low-E Kaons), or from underestimated number of neutrino events in both neutrino and anti-neutrino runs (ν scaled).

From the simple comparison given in Table 3 one can see that the hypothesis with the highest

Hypothesis	Stat Only	Cor. Syst	Uncor. Syst	Number ν Expec.
POT scaled	0.0%	0.0%	1.8%	67.5
Same ν,$\bar{\nu}$ NC	0.1%	0.1%	6.7%	37.2
NC π^0 scaled	3.6%	6.4%	21.5%	19.4
Bkgd scaled	2.7%	4.7%	19.2%	20.9
CC scaled	2.9%	5.2%	19.9%	20.4
Low-E Kaons	0.1%	0.1%	5.9%	39.7
ν scaled	38.4	51.4%	58.0%	6.7

Table 3: The χ^2 probability assuming one degree of freedom for testing various hypotheses (described in the text) as an explanation of the low energy events in neutrino and anti-neutrino modes.

probability is the one where the low energy excess originates from only neutrinos in the beam. However, more rigorous analysis of the low energy excess, currently underway, is needed to make a strong statement on the nature of the low energy excess. As of June 2009, the MiniBooNE experiment has collected a total of 5.0×10^{20} POT, and has been approved for further running to collect a total of 10.0×10^{20} POT in anti-neutrino mode.

4 MiniBooNE NuMI Results

An additional data sample measured by the MiniBooNE detector comes from neutrinos produced in the NuMI (Neutrinos from Main Injector) beam line. Fermi National Accelerator Laboratory has two beam lines that produce neutrinos: the Booster Neutrino Beam (BNB) and the NuMI beam line, as shown in Fig. 3. The BNB beam is designed for use by the MiniBooNE experiment. The NuMI beam produces neutrinos for the MINOS experiment. However, the MiniBooNE detector observes neutrinos from the NuMI beamline, at an off-axis angle of 6.3 degrees. The

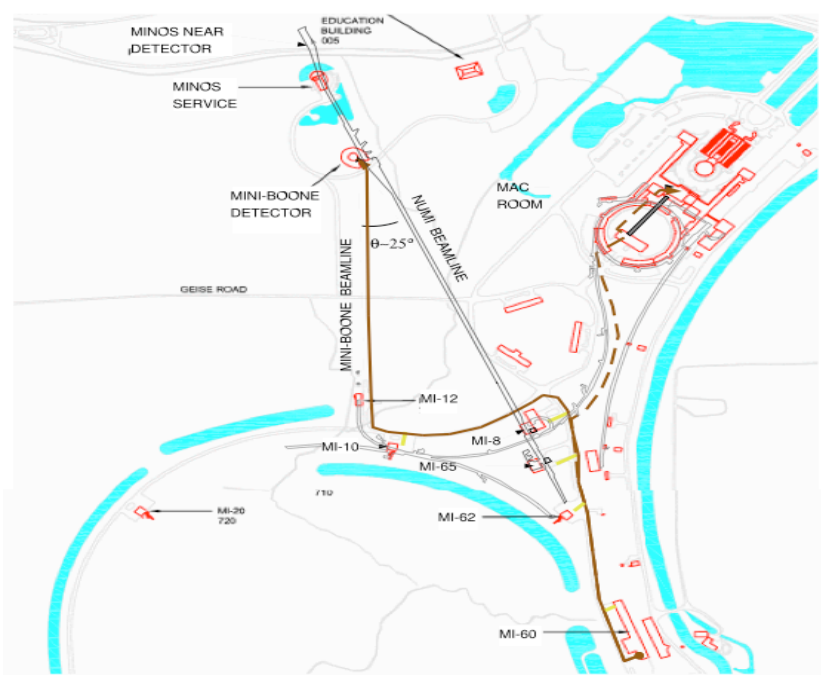

Figure 3: Fermi Nation Accelerator Laboratory is currently running two beam lines that produce neutrinos. The BNB produces neutrinos used in the MiniBooNE experiment. The NuMI Beam is emitting neutrinos intended for use in the MINOS experiment.

NuMI neutrino flux at the MiniBooNE detector is shown in Fig. 4. Samples of charged current

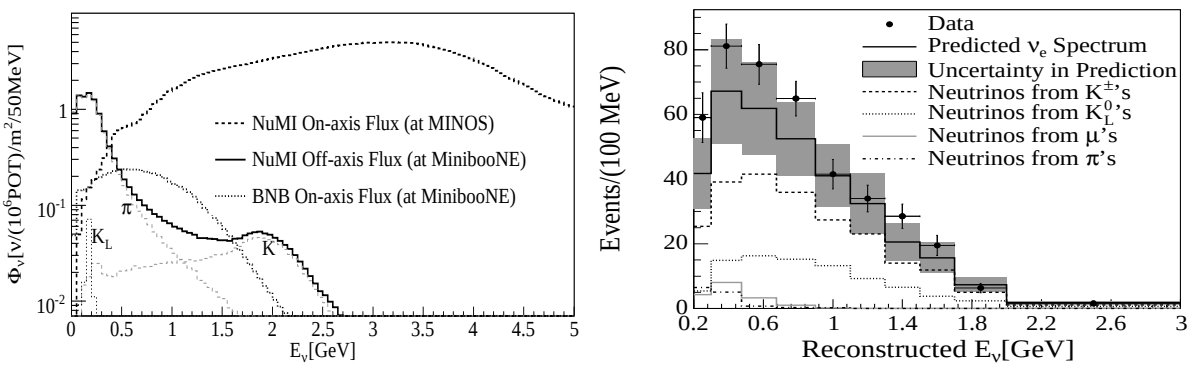

Figure 4: Left: Comparison of the predicted NuMI off-axis, NuMI on-axis, and MiniBooNE fluxes including all neutrino species. The off-axis flux is separated into contributions from charged π and K parents. Right: Reconstructed E_ν distribution of the NuMI off-axis ν_e CCQE candidate events in MiniBooNE. The prediction is separated into contributions from neutrino parents. The band indicates the total systematic uncertainty associated with the MC prediction. Kaon parents contribute 93% of the events in this sample.

quasi-elastic (CCQE) ν_μ and ν_e interactions were analyzed. The high rate and simple topology of ν_μ CCQE events provided a useful sample for understanding the ν_μ spectrum and verifying the MC prediction for ν_e production. The ν_e CCQE sample energy distribution is shown in Fig. 4. These results are described elsewhere [12,13] and show that reliable predictions for an off-axis beam can be made.

After the demonstration of the off-axis concept, useful in limiting backgrounds in searches for the oscillation transition $\nu_\mu \rightarrow \nu_e$, the analysis is directed toward examing the low energy region and searching for oscillation. In this way it complements the analysis done at MiniBooNE using the BNB neutrino and anti-neutrino BNB, but with different systematics. The phenomenological interpretations of the MiniBooNE results, already mentioned, as well as the excess of events observed in neutrino mode and the lack of excess in anti-neutrino mode, have provided additional motivation for a neutrino appearance search at MiniBooNE using neutrinos from the NuMI beamline. It is important to note that the NuMI ν_e CCQE sample has a very different composition when compared to the BNB neutrino ν_e CCQE sample. The BNB ν_e sample originates mostly from decays of pions produced in the target, and contains large fraction of ν_μ mis-identified events. The NuMI ν_e CCQE sample is produced mostly from the decay of kaons, and contains a dominant fraction of intrinsic ν_e events.

The analysis will be performed by forming a correlation between the large statistics ν_μ CCQE sample and ν_e CCQE, and by tuning the prediction to the data simultaneously. Considering various sources of systematic uncertainty, a covariance matrix in bins of E_ν is constructed, which includes correlations between ν_e CCQE (oscillation signal and background) and ν_μ CCQE samples. This covariance matrix is used in the χ^2 calculation of the oscillation fit. The result is that the prediction is being constrained, i.e. tuned to the data, and common systematic components in ν_e and ν_μ CCQE samples cancel. The cancellation results from the fact that the majority of the events in both ν_e and ν_μ CCQE samples originate from pure charged current interaction of neutrinos sharing same parent mesons, effectively sharing same cross-section and beam systematic components. This is a method equivalent to forming a ratio between near and far detectors in two-detector experiments where the near detector detects ν_μ CCQE events, while the far detector samples ν_e CCQE events. This analysis is in a preliminary stage and is expected to be completed in the near future.

5 Conclusion

MiniBooNE observed an unexplained excess of electron-like events in the low energy region in neutrino mode. However, no excess of such events is observed so far at low energies in anti-neutrino mode. MiniBooNE was approved for additional running in anti-neutrino mode, to collect a total of 10×10^{20} protons on target. With this additional data taking, which should continue through 2011, as well as with the NuMI neutrinos measured by MiniBooNE the collaboration will be in a position to determine whether there is an anomalous difference between neutrino and anti-neutroino properties.

Acknowledgments

I would like to acknowledge the support of Fermilab, the Department of Energy, and the National Science Foundation.

References

1. C. Athanassopoulos *et al.*, Phys. Rev. D 64 (2001) 112007.
2. A. A. Aguilar-Arevalo *et al.*, Phys. Rev. Lett. **98**, 231801 (2007).
3. A. A. Aguilar-Arevalo *et al.*, Phys.Rev.Lett. **102**, 101802 (2009) ,arXiv:0812.2243 [hep-ex].
4. Michel Sorel, Janet Conrad, and Michael Shaevitz, Phys. Rev. D **70**, 073004 (2004); G. Karagiorgi *et al.*, Phys. Rev. D **75**, 013011 (2007); Alessandro Melchiorri *et al.*, [arXiv:0810.5133]; Michele Maltoni and Thomas Schwetz, Phys. Rev. D **76**, 093005 (2007); G. Karagiorgi, Z. Djurcic, J. M. Conrad, M. H. Shaevitz and M. Sorel, sumbitted to Phys. Rev. D, arXiv:0906.1997.
5. Jeffrey A. Harvey, Christopher T. Hill, and Richard J. Hill, Phys. Rev. Lett. **99**, 261601 (2007); Phys. Rev. D **77**, 085017 (2008).
6. Heinrich Paes, Sandip Pakvasa, and Thomas J. Weiler, Phys. Rev. D **72**, 095017 (2005).
7. T. Goldman, G. J. Stephenson Jr., and B. H. J. McKellar, Phys. Rev. D **75**, 091301 (2007).
8. Ann E. Nelson and Jonathan Walsh, Phys. Rev. D **77**, 033001 (2008).
9. S. Hollenberg, O. Micu, H. Pas, arXiv:0906.5072 [hep-ph].
10. A. A. Aguilar-Arevalo *et al.*, Phys. Rev. D **78**, 012007 (2008), arXiv:0805.1764 [hep-ex].
11. A. A. Aguilar-Arevalo *et al.*, arXiv:0904.1958 [hep-ex].
12. Z. Djurcic, talk given at International Conference on High Energy Physics (ICHEP08), Philadelphia, 2008, arXiv:0901.1648 [hep-ex].
13. P. Adamson *et al.*, Phys. Rev. Lett. **102**, 211801 (2009), arXiv:0809.2447 [hep-ex].